Jordan et al., http://www.jcb.org/cgi/content/full/jcb.201510063/DC1

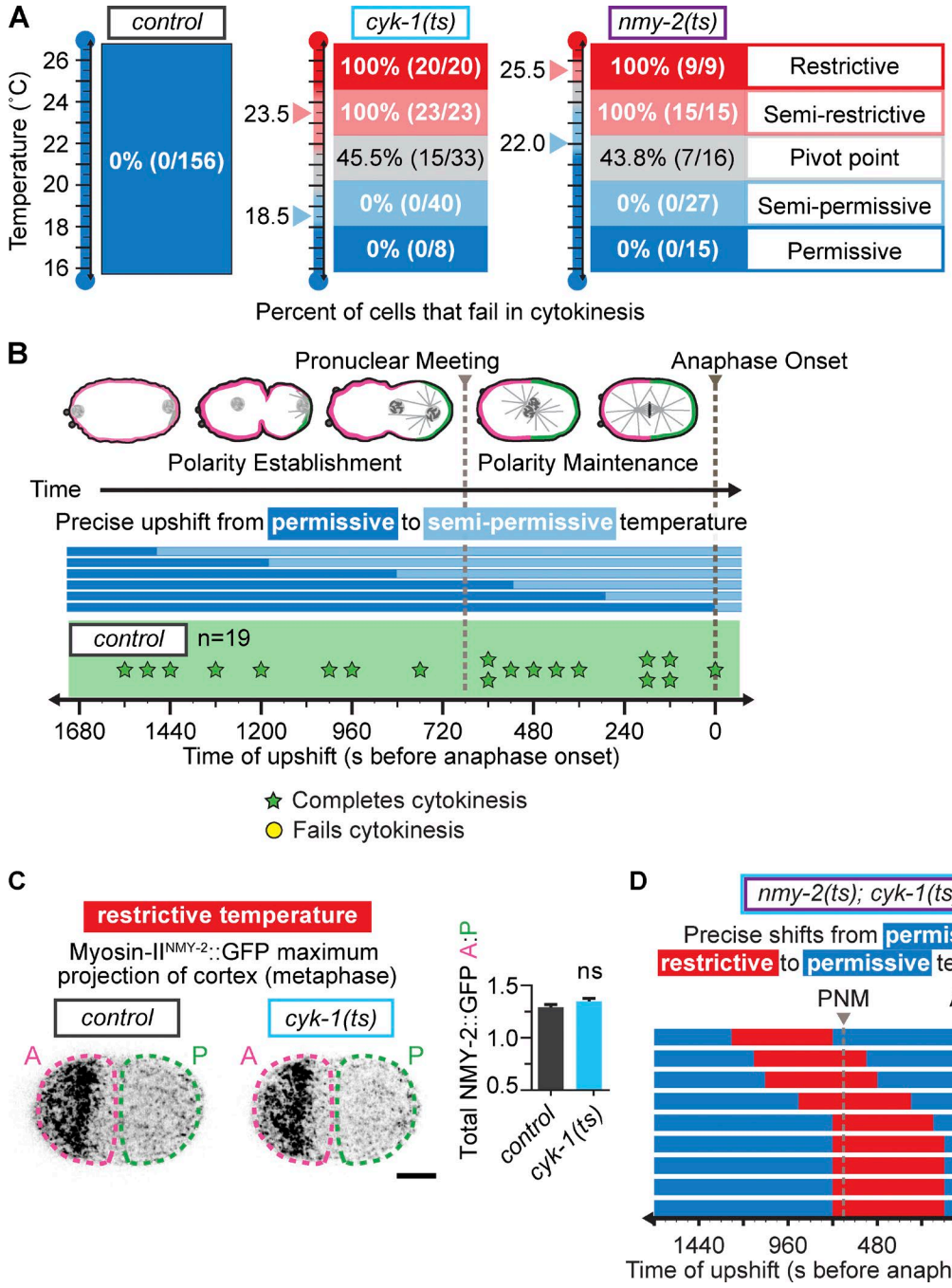

Figure S1. **ts mutants allow tuning of specific protein functions that are necessary for cytokinesis.** (A) Temperature response tables for control, *formin(ts)*, and *myosin-II(ts)* embryos. Formin and myosin-II fast-acting ts mutants have tunable constriction defects dependent on temperature. (B) Control embryos complete cytokinesis when upshifted to a semipermissive temperature before cytokinesis. (C) At fully restrictive temperature, *formin(ts)* embryos successfully polarize myosin-II (NMY-2::GFP) in an anterior cap before cytokinesis. ns, not significant. Error bars represent SD. (D) Double *myosin-II(ts);formin(ts)* mutant embryos complete cytokinesis when temporarily upshifted to restrictive temperature and returned to a fully permissive temperature before anaphase onset (AO), indicating that these ts mutant phenotypes are reversible. PNM, pronuclear meeting. Bar, 10 µm. *cyk-1* = *formin*; *nmy-2* = *myosin-II*.

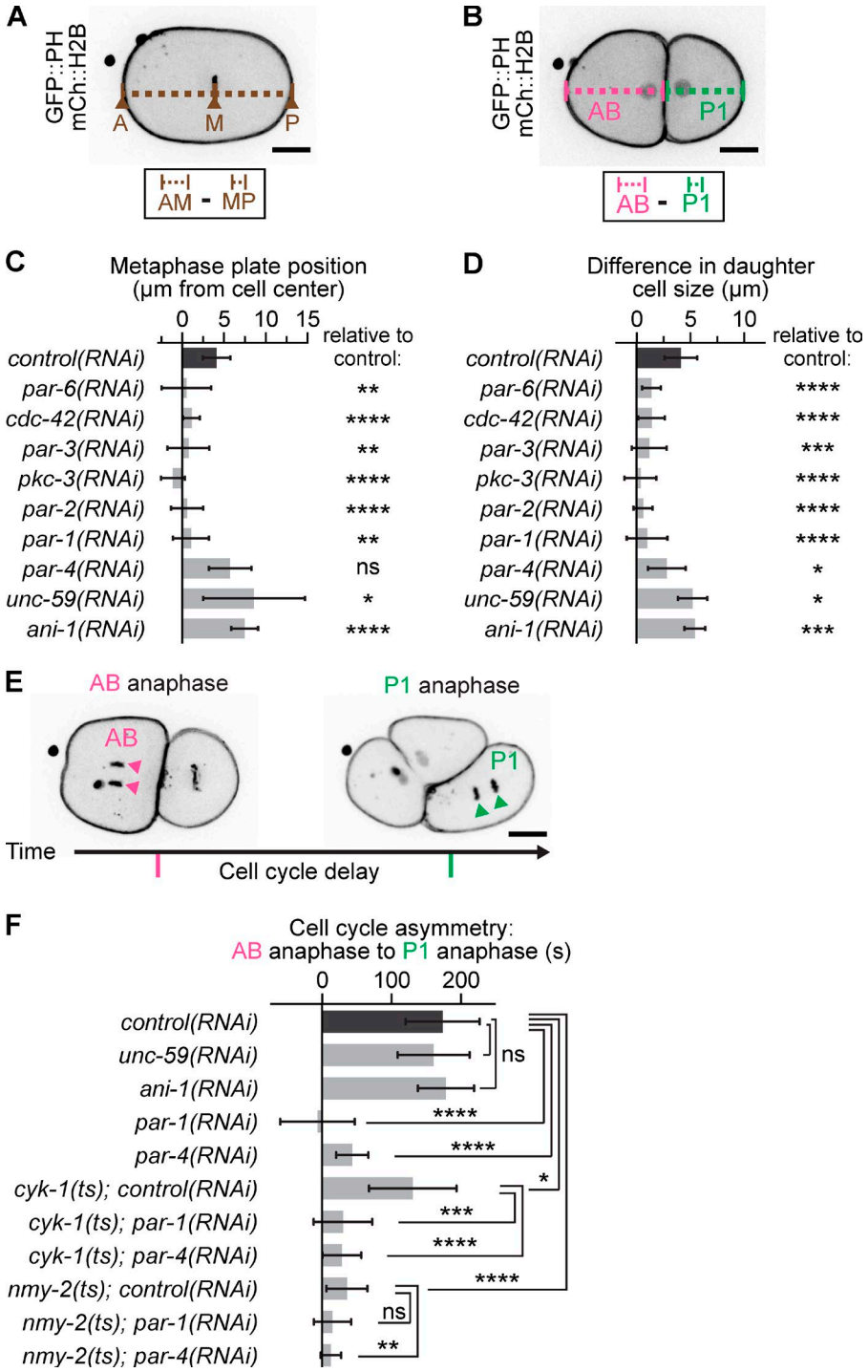

Figure S2. **Successful RNAi-mediated knockdown of PAR proteins was confirmed using hallmarks of the loss of polarity.** (A) Metaphase plate (m) position in RNAi-depleted embryos was measured immediately before anaphase onset by calculating the deviation in position of the metaphase plate from the cell center (at 0 µm) toward the anterior (negative change) or posterior (positive change). (B) Daughter cell size asymmetry was measured immediately after contractile ring closure. Asymmetric division is indicated by an increased difference in daughter cell length (when AB > P1). (C) Metaphase plate position for RNAi-depleted embryos. (D) Daughter cell size asymmetry for RNAi-depleted embryos. (E) Successful depletion of cytoplasmic polarity regulators (PAR-1 and PAR-4) was determined by measuring the loss of the cell cycle delay between anaphase onset in the AB blastomere and anaphase onset in the P1 blastomere. In control embryos, there is a significant delay between the two cell cycles; this difference is lost upon disruption of cytoplasmic polarity. (F) Difference in time between anaphase of AB and anaphase of P1. All data are shown as mean ± SD. *, $P < 0.05$; **, $P < 0.005$; ***, $P < 0.0005$; ****, $P < 0.0001$; ns, not significant. Bars, 10 µm. *cyk-1 = formin; nmy-2 = myosin-II; unc-59 = septin; ani-1 = anillin.*

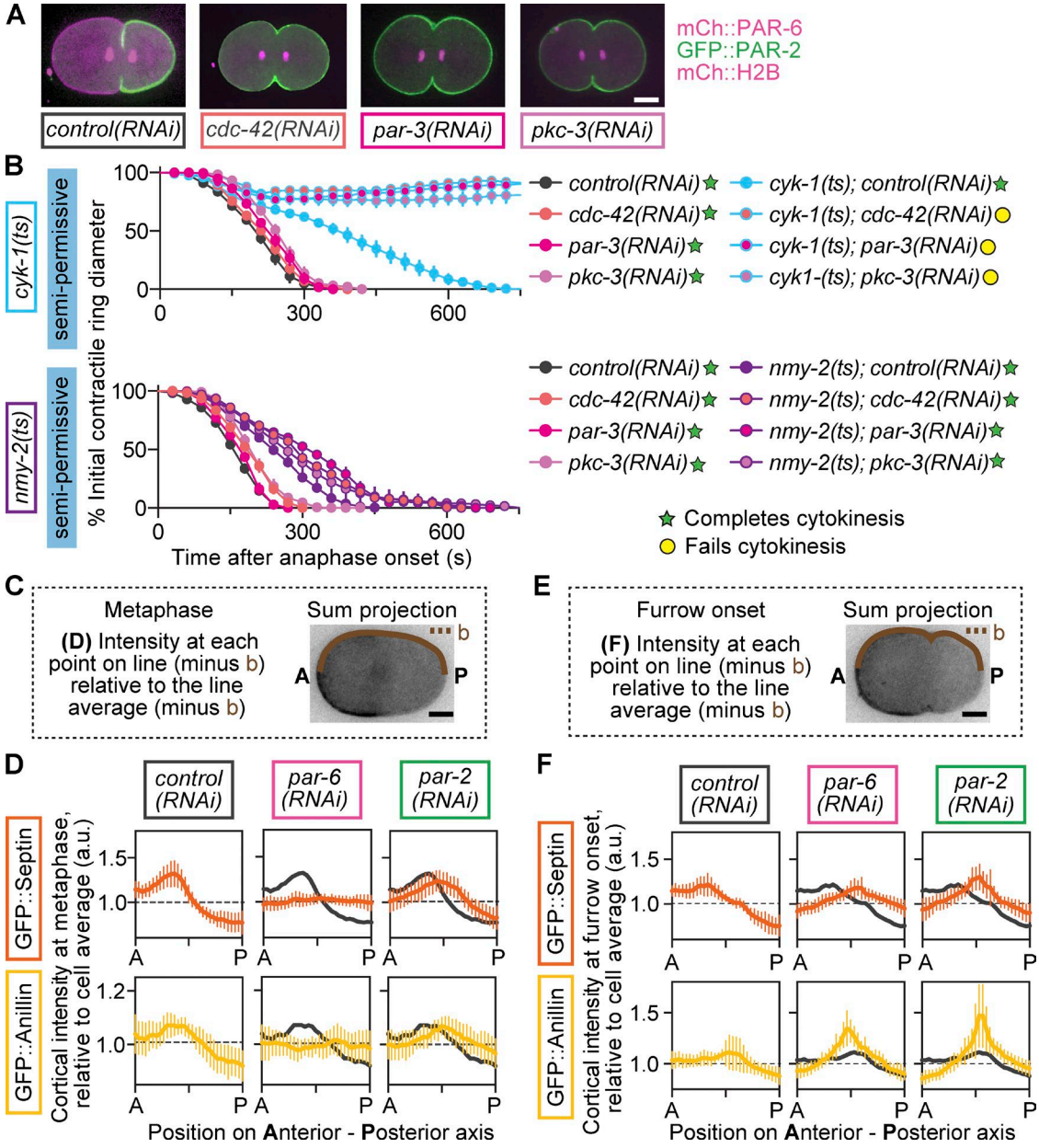

Figure S3. **Cortical PAR proteins regulate cytokinesis and sequester septin and anillin in the cell anterior.** (A) Depletion of the aPAR proteins CDC-42, PAR-3, and PKC-3 results in an expansion of the pPAR protein PAR-2 into the entire cell cortex. (B) RNAi-mediated depletion of cortical aPAR proteins (CDC-42, PAR-3, or PKC-3) leads to cytokinesis failure in *formin(ts)* but not *myosin-II(ts)* mutant embryos at semipermissive temperature ($n \geq 9$, all conditions; mean ± SEM). (C) Schematic of line scan taken for quantifications in D to measure reporter localization. (D) At metaphase, septin and anillin are enriched in the cell anterior in a PAR-dependent manner ($n \geq 10$, all conditions; mean ± SD). (E) Schematic of line scan taken for quantifications in F to quantify reporter localization. (F) At furrow onset, septin and anillin are enriched in the cell anterior in a PAR-dependent manner ($n \geq 10$, all conditions; mean ± SD). (D and F) Mean from *control(RNAi)* is displayed for reference. Bars, 10 µm. a.u., arbitrary units; b, background. *cyk-1* = *formin*; *nmy-2* = *myosin-II*.

Table S1. **Strain names and genotypes**

Strain	Genotype
OD95	*unc-119(ed3)*[a] *ltIs38 [pAA1; pie-1/GFP::PH(PLC1delta1); unc-119 (+)]III; ltIs37 [pAA64; pie-1/mCHERRY::his-58; unc-119(+)]IV*
JCC146	*cyk-1(or596ts) unc-119(ed3)*[a] *ltIs38 [pAA1; pie-1/GFP::PH(PLC1delta1); unc-119(+)]III; ltIs37 [pAA64; pie-1/mCHERRY::his-58; unc-119(+)]IV*
JCC192	*nmy-2(ne3409ts) dpy-5*[b] *I; unc-119(ed3)*[a] *ltIs38 [pAA1; pie-1/GFP::PH(PLC1delta1); unc-119(+)]III; ltIs37 [pAA64; pie-1/mCHERRY::his-58; unc-119(+)]IV*
JCC212	*nmy-2(ne3409ts) dpy-5*[b] *I; cyk-1(or596ts) unc-119(ed3)*[a] *ltIs38 [pAA1; pie-1/GFP::PH(PLC1delta1); unc-119(+)]III; ltIs37 [pAA64; pie-1/mCHERRY::his-58; unc-119(+)]IV*
JCC744	*unc-119(ed3)*[a] *III; ddIs25 [GFP::F58B6.3;unc-119(+)]; ddIs26 [mCherry::T26E3.3;unc-119(+)]; ltIs37 [pAA64; pie-1/mCHERRY::his-58; unc-119(+)]IV*
JCC719	*mgSi3[cb-unc-119(+); GFP:UTROPHIN]II; unc-119(ed3)*[a] *III; ltIs37 [pAA64; pie-1/mCHERRY::his-58; unc-119(+)]IV*
JCC541	*unc-119(ed3)*[a] *III; ltIs37 [pAA64; pie-1/mCHERRY::his-58; unc-119 (+)] IV; zuIs45[nmy-2::NMY-2::GFP; unc-119(+)]V*
JCC559	*cyk-1(or596ts) unc-119(ed3)*[a] *III; ltIs37 [pAA64; pie-1/mCHERRY::his-58; unc-119(+)] IV; zuIs45[nmy-2::NMY-2::GFP; unc-119(+)] V*
JCC425	*unc-119(ed3)*[a] *III; ltIs37 [pAA64; pie-1/mCHERRY::his-58; unc-119(+)] IV; ltIs20 [pASM10; pie-1:GFP::unc-59; unc-119(+)]*
OD159	*unc-119(ed3)*[a] *III; ltIs86 [pASM65; pie-1:ani-1(fl cDNA)::GFP; unc-119(+)]*

[a]The unc-119(ed3) mutation was present in the parental strains but has not been directly sequenced in these strains to determine if the unc-119 gene is mutated.
[b]The exact dpy-5 allele is unknown but presumed to be e61, as published in Carvalho et al. (2009).

Table S2. **Feeding RNAi constructs**

Plasmid	Gene(s)	Oligo 1 (5′-3′)	Oligo 2 (5′-3′)	Template	Cloning Vector
pJC165	*par-1* (*H39E23.1*)	gcgcgACTAGTttgctgattttggattttcg	gcgcgACTAGTgctgatcctgcagtgattgat	N2 cDNA	L4440 (empty vector)
pJC317	*par-2* (*F58B6.3*)	gcgcgACTAGTcggccgctctagaactagtat	gcgcgACTAGTtcctgcagcccgggggat	N2 cDNA	L4440
pJC166	*pkc-3* (*F09E5.1*)	gcgcgACTAGTcgtctccgacatcattagagg	gcgcgACTAGTgattcggtctggaagcaaga	N2 cDNA	L4440
pJC186	*par-4* (*Y59A8B.14*)	gcgcgACTAGTgggccgtcaaaattatgaaat	gcgcgACTAGTaggccttgatcctctggg	N2 cDNA	L4440
pJC132	*ani-1* (*Y49E10.19*)	gcgcgACTAGTactccagtgcattttcaccc	gcgcgACTAGTgacgatgatgatgatgtcgc	N2 cDNA	L4440
pJC43	*par-3* (*F54E7.3*)	Acquired from Ahringer library (Clone # III-3A01)			
pJC56	*par-6* (*T26E3.3*)	Acquired from Ahringer library (Clone # I-6M10)			
pJC53	*cdc-42* (*R07G3.1*)	Acquired from Ahringer library (Clone # II-5P13)			
pJC55	*unc-59* (*W09C5.2*)	Acquired from Ahringer library (Clone # I-6N04)			
pJC319	*par-2* (*F58B6.3*) and *unc-59* (*W09C5.2*)	gcgcgGAATTCcggccgctctagaactagtat	gcgcgGAATTCtcctgcagcccgggggat	pJC317 (par-2)	pJC55 (unc-59)
pJC318	*par-6* (*T26E3.3*) and *unc-59* (*W09C5.2*)	gcgcgGAATTCgaaaaatccaaattttca	gcgcgGAATTCttaacgatttttgagctgt	pJC56 (par-6)	pJC55 (unc-59)

This table details the feeding RNAi constructs used in this study, including plasmid names, targeted genes for RNAi experiments, oligos used to generate RNAi feeding construct and DNA template used or Ahringer library (Kamath and Ahringer, 2003; Kamath et al., 2003) clone number, and cloning vectors used in this study.

References

Carvalho, A., A. Desai, and K. Oegema. 2009. Structural memory in the contractile ring makes the duration of cytokinesis independent of cell size. *Cell*. 926–937. http://dx.doi.org/10.1016/j.cell.2009.03.021

Kamath, R.S., and J. Ahringer. 2003. Genome-wide RNAi screening in *Caenorhabditis elegans*. *Methods.* 30:313–321. http://dx.doi.org/10.1016/S1046-2023(03)00050-1

Kamath, R.S., A.G. Fraser, Y. Dong, G. Poulin, R. Durbin, M. Gotta, A. Kanapin, N. Le Bot, S. Moreno, M. Sohrmann, et al. 2003. Systematic functional analysis of the *Caenorhabditis elegans* genome using RNAi. *Nature.* 421:231–237. http://dx.doi.org/10.1038/nature01278